Numerical investigation of the propagation of shock waves in rigid porous materials

Solution of the Riemann problem

G. Ben-Dor and A. Levy
Pearlstone Center for Aeronautical Engineering Studies, Ben-Gurion University of the Negev, Beer Sheva, Israel, and
S. Sorek
J. Blaustein Desert Research Institute, Ben-Gurion University of the Negev, Sede Boker, Israel

Received September 1995
Revised August 1996

Introduction

A detailed investigation of the head-on collision of planar shock waves with rigid[1] porous materials was initiated on the theoretical basis of macroscopic balance equations. The macroscopic mass, momentum and energy balance equations, for a saturated porous medium, were developed by Levy *et al.* (1995) by conducting a dimensional analysis on the macroscopic balance equations of Bear *et al.* (1992) and Sorek *et al.* (1992). It is novel in establishing the macroscopic theoretical basis for non-linear wave motion in multi-phase deformable porous media. The modelling is based on conceptualizing the porous medium as a continuum composed of interacting compressible solid and a fluid phases (saturated porous media). Macroscopic physical laws expressing mass, momentum and energy balances for fluid and the solid matrix are formulated on the basis of representative elementary volume (REV) concepts, presented by Bear and Bachmat (1990). These macroscopic balance equations are composed of averaged flux terms together with integrals of microscopic exchange flux terms at the solid-fluid interface. Some unique macroscopic parameters which arise from the averaging process are the tortuosity factor which represents a tensor associated with the matrix directional cosines, the hydraulic radius of the pore spaces and the porosity which represents the volume fraction of the pores filled by the fluid. Note that unlike models developed in the past (e.g. Baer, 1988), which account only for the properties of the phases, the macroscopic model developed in the course of this study also accounts for geometrical properties. Hence, in addition, the speed of the wave is also a function of the porous material structure. Unlike Bear and Bachmat (1990), Levy *et al.* (1995a) showed that a Forchheimer term should be included as an additional macroscopic inertia term commencing from the microscopic inertia exchange between the phases at the solid-fluid interface.

A dimensional analysis was applied to the macroscopic balance equations of the phases after the simultaneous onset of an abrupt change of the pressure and

International Journal of Numerical Methods for Heat & Fluid Flow
Vol. 7 No. 8, 1997, pp. 801–813.

temperature of the fluid. Levy *et al.* (1995a) obtained four significant evolution periods. In the first evolution period, pressure, temperature and stress are spatially distributed without attenuation. The vertical stress, however, is linearly dependent on gravity. In the second evolution period, they noted the rise of non-linear wave forms. In the third evolution period, the inertial and dissipation terms were found to be of the same order and consequently, the entire macroscopic Navier-Stokes equations should be considered. In the fourth evolution period, the inertial terms were found to be negligible in comparison to the dissipation terms. Assuming that the friction between the solid and the fluid is higher than the one between the fluid layers, the non-linear Darcy law (i.e. including Forchheimer term) for momentum balance equation of the fluid is obtained.

In a following study, Levy *et al.* (1995b) developed a macroscopic 1-D analytical model for describing compaction wave propagation in rigid porous media. Unlike Krylov *et al.* (1996) and Sorek *et al.* (1996) who neglected the momentum and energy exchanges between the two phases and assumed that the coupling between them was only owing to the effective stress, in this study the momentum and energy exchanges between the two phases was also accounted for. Based on the dimensional analysis of Levy *et al.* (1995a), who showed that the linear Darcy term was much smaller than the non-linear Forchheimer term, only the Forchheimer term appeared in the momentum and energy exchanges between the two phases. In addition, it was assumed in this model that both the porosity and the temperature of the solid phase remain constant and that the inertial force of the solid phase is negligibly small.

As part of the investigation, it was decided to solve numerically the full one-dimensional set of the governing equations as developed and presented by Levy *et al.* (1995a). A TVD-based computer code for solving the governing equations was developed by Levy *et al.* (1996b). Its predictions were compared to experimental results and very good to excellent agreement was evident. Many more details can be found in Levy (1995).

As a consequence of the numerical study it was decided to solve the simple shock tube problem, i.e. the Riemann problem (see Figure 1) for the case in which the media in both sides of the diaphragm are porous. To the best of the authors' knowledge, such a solution has not been conducted yet. Neither had the compaction waves been simulated in a porous medium.

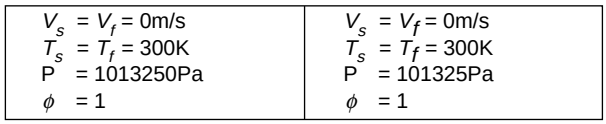

Note that ϕ = 1 implies that the entire medium consists of only a gaseous phase

(a)

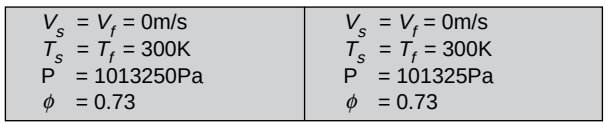

$E_\varepsilon = 380.10^7$Pa, $E_T = 26.207$Kg/m^3, $F = 300$l/m, $T^* = 0.7$ and $\rho_s = 2030$Kg/m^3

(b)

Figure 1.
Schematic illustration of the two problems solved in the course of the present study (a) The Riemann problem in a pure gas (b) The Riemann problem in a porous medium

Present study

Owing to the fact that detailed derivation of the governing equations can be found in the above mentioned publications which resulted from our investigation, in the following, only the final form of the one-dimensional governing equations and the assumptions on which their derivation was based are presented.

The assumptions

The following assumptions are made:

- The fluid is ideal (i.e. $\mu_f = 0$ and $\lambda_f = 0$ where μ_f is the dynamic viscosity and λ_f is the thermal conductivity).
- The fluid is a perfect gas.
- The dispersive and diffusive mass fluxes of the fluid, and the dispersive flux of the solid, are much smaller than the corresponding advective ones and may, therefore, be neglected.
- The dispersive flux of momentum is much smaller than its advective one and may, therefore, be neglected.
- The microscopic solid-fluid interfaces are material surfaces with respect to the mass of both phases.
- The solid matrix is thermoelastic, and is assumed to undergo small deformations only.
- The stress-strain relationship for the solid, at the microscopic level, and for the solid matrix, at the macroscopic level, have the same form.
- The material of which the skeleton of the porous material is made is incompressible.
- The specific heats at constant volume, C_f, and that at constant strain, C_s, for the solid, are constant.
- The energy processes for the fluid and for the solid are reversible.
- There are no external energy sources.
- The energy associated with viscous dissipation is negligibly small.
- The conductive and dispersive heat fluxes of the phases are negligibly small when compared to their advective heat flux.
- The rate of heat transferred between the fluid and solid phases is negligibly small.

The one-dimensional governing equations

In a vector form the one-dimensional version of the governing equations are as follows:

$$\frac{\partial \mathbf{U}}{\partial t} + \frac{\partial \mathbf{F}}{\partial x} = \mathbf{Q} \tag{1}$$

The variables vector, **U**, is defined by

$$\mathbf{U} = \left[\rho_f, \quad \rho_s, \quad m_f, \quad m_s, \quad E_f, \quad E_s\right]^T \tag{2}$$

where

$$\rho_f \equiv \phi\rho_f \quad , \quad m_f \equiv \rho_f V_f \quad , \quad \rho_s \equiv (1-\phi)\rho_s \quad , \quad m_s \equiv \rho_s V_s$$

$$E_f \equiv \rho_f e_f = \rho_f\left(C_f T_f + \frac{V_f^2}{2}\right) \quad , \quad E_s \equiv \rho_s e_s = \rho_s\left(C_s T_s + \frac{V_s^2}{2}\right) \tag{3}$$

where ρ_α, V_α and T_α denotes the density, the velocity and the temperature of the α-phase ($\alpha \equiv f,s$) respectively. C_α denotes its specific heat capacity at constant volume and T^* denote the tortuosity coefficient of the fluid phase.

The flux vector, **F**, is

$$\mathbf{F} = \begin{bmatrix} m_f \\ m_s \\ \dfrac{m_f^2}{\rho_f} + T^*\phi P \\ \dfrac{m_s^2}{\rho_s} - \sigma_s' + \left(1-\phi T^*\right)P \\ \dfrac{m_f}{\rho_f}\left(E_f + T^*\phi P\right) \\ \dfrac{m_s}{\rho_s}\left(E_s - \sigma_s' + \left(1-\phi T^*\right)P\right) \end{bmatrix} \tag{4}$$

The source vector, **Q**, is

$$\mathbf{Q} = \begin{bmatrix} 0 \\ 0 \\ T^*P\dfrac{\partial\phi}{\partial x} - \tilde{F}\rho_f\left|\dfrac{m_f}{\rho_f} - \dfrac{m_s}{\rho_s}\right|\left(\dfrac{m_f}{\rho_f} - \dfrac{m_s}{\rho_s}\right) \\ -T^*P\dfrac{\partial\phi}{\partial x} + \tilde{F}\rho_f\left|\dfrac{m_f}{\rho_f} - \dfrac{m_s}{\rho_s}\right|\left(\dfrac{m_f}{\rho_f} - \dfrac{m_s}{\rho_s}\right) \\ \dfrac{m_s}{\rho_s}\left(T^*P\dfrac{\partial\phi}{\partial x} - \tilde{F}\rho_f\left|\dfrac{m_f}{\rho_f} - \dfrac{m_s}{\rho_s}\right|\left(\dfrac{m_f}{\rho_f} - \dfrac{m_s}{\rho_s}\right)\right) \\ \dfrac{m_s}{\rho_s}\left(-T^*P\dfrac{\partial\phi}{\partial x} + \tilde{F}\rho_f\left|\dfrac{m_f}{\rho_f} - \dfrac{m_s}{\rho_s}\right|\left(\dfrac{m_f}{\rho_f} - \dfrac{m_s}{\rho_s}\right)\right) \end{bmatrix} \tag{5}$$

where ϕP and the effective stress, σ_s', which appear in (4) are defined as follows:

$$\phi P = (\gamma - 1)\left[E_f - \frac{m_f^2}{2\rho_f}\right] \quad , \tag{6}$$

$$\sigma_s' = E_\varepsilon \varepsilon - E_T C_s (T_s - T_{s0}) \quad , \tag{7}$$

In the above equations $E_\varepsilon (\equiv \lambda_s'' + \mu_s')$ and $E_T (\equiv \eta / C_s)$ are the one-dimensional macroscopic coefficients which associate with the Lame's coefficients, μ_s', λ_s'' and η, for a thermoelastic solid. With the aid of definitions (3) the porosity, ϕ, can be written as

$$\phi = 1 - \frac{r_s}{\rho_s} \tag{8}$$

The strain, ε, can be expressed as a function of the porosity as

$$\varepsilon = 1 - \frac{r_s}{r_{s_0}} \tag{9}$$

With the aid of (3), equation (7) can be rewritten as

$$\sigma_s = E_\varepsilon \left(\frac{r_{s0} - r_s}{r_{s0}} \right) - E_T \left(\frac{E_s}{r_s} - \frac{E_{s0}}{r_{s0}} - \frac{m_s^2}{2r_s^2} + \frac{m_{s0}^2}{2r_{s0}^2} \right) \tag{10}$$

The above set of equations consists of six differential equations, described by equations (1) and (2), and six unknowns namely: r_f, r_s, m_f, m_s, E_f and E_s. Consequently, in principle, the equations are complete and can be solved. However, owing to the complexity of the equations, an analytical solution of the set is impossible. Note that simplified cases were solved analytically by Levy *et al.* (1995b; 1996), Krylov *et al.* (1996) and Sorek *et al.* (1996). Some of these solutions were verified by comparison with experimental results. Instead, a numerical solution has been performed in the present study, Details of the numerical method are given in the next section.

Note that in writing equation (1) we assumed that the gradients of the porosity were very small and therefore they might be written as source terms in the source vector, **Q**, given by (5). As a result the source vector, **Q**, contains derivative terms and thus affects the character of the equations (hyperbolic rather then elliptic-hyperbolic). This is very convenient for numerical purposes and is correct only when the gradients of the porosity are very small, as is the case in this study. Applying this procedure removes the ill-posedness associated with the elliptic-hyperbolic character of the equations which is usually manifested in highly oscillatory solutions as the mesh is refined.

The numerical method

An upwind TVD shock-capturing scheme, originally developed by Harten (1983), was extended to solve the problem of two phase flow which described waves propagation and interaction in saturated porous media. The scheme for solving equation (1) can be written in the following conservative form

$$\mathbf{U}_j^{n+1} = \mathbf{U}_j^n - \lambda \left(\overline{\mathbf{F}}_{j+1/2} - \overline{\mathbf{F}}_{j-1/2} \right) + \Delta t \mathbf{Q}_j \tag{11}$$

where the parameter λ is defined by

$$\lambda \equiv \Delta t / \Delta x \tag{12}$$

and the numerical flux, $\overline{\mathbf{F}}_{j+1/2}$, is evaluated from

$$\overline{\mathbf{F}}_{j+1/2} = \frac{1}{2}\left[\mathbf{F}\left(\mathbf{U}_j^n\right) + \mathbf{F}\left(\mathbf{U}_{j+1}^n\right) - \frac{1}{\lambda}\sum_{k=1}^{6}\beta_{j+1/2}^k \mathbf{R}_{j+1/2}^k\right] \tag{13}$$

$$\beta_{j+1/2}^k = \Psi^k\left(\nu_{j+1/2}^k + \gamma_{j+1/2}^k\right)\alpha_{j+1/2}^k - \left(g_j^k + g_{j+1}^k\right) \tag{14}$$

$$\nu_{j+1/2}^k = \lambda a^k\left(\mathbf{U}_{j+1/2}\right) \tag{15}$$

$$\gamma_{j+1/2}^k = \begin{cases} \left(g_{i+1}^k - g_i^k\right)/\alpha_{j+1/2}^k & \alpha_{j+1/2}^k \neq 0 \\ 0 & \alpha_{j+1/2}^k = 0 \end{cases} \tag{16}$$

$$g_i^k = \operatorname{sgn}\left(\tilde{g}_{j+1/2}^k\right)\max\left[0, \min\left(\left|\tilde{g}_{j+1/2}^k\right|, \tilde{g}_{j-1/2}^k \operatorname{sgn}\left(\tilde{g}_{j+1/2}^k\right)\right)\right] \tag{17}$$

$$\tilde{g}_{j+1/2}^k = \frac{1}{2}\left[y^k\left(v_{j+1/2}^k\right) - \left(v_{j+1/2}^k\right)^2\right]a_{j+1/2}^k \tag{18}$$

$$\Psi(x) = \begin{cases} x^2/4\xi + \xi & |x| < 2\xi \\ |x| & |x| \geq 2\xi \end{cases}$$
$$\xi = \begin{cases} 0.1 & \left(\partial a^k/\partial \mathbf{U}\right)\mathbf{R}^k \neq 0 \\ 0 & \left(\partial a^k/\partial \mathbf{U}\right)\mathbf{R}^k = 0 \end{cases} \tag{19}$$

The eigenvalues, a^k, of the Jacobian matrix $\mathbf{A}(\mathbf{U}) = \partial\mathbf{F}/\partial\mathbf{U}$ were found symbolically by using the application *Mathematica* to be

$$a^1 = V_s - a_s \;\; ; \;\; a^2 = V_f - a_f \;\; ; \;\; a^3 = V_s$$
$$a^4 = V_f \;\; ; \;\; a^5 = V_f + a_f \;\; ; \;\; a^6 = V_s + a_s \tag{20}$$

where a_f and a_s are the equivalent speeds of sound of the fluid and the solid phases respectively.

They can be expressed as

$$a_f^2 = \frac{\phi P\left(1 - T^* + \gamma T^*\right)T^*}{r_f} \tag{21}$$

and

$$a_s^2 = \frac{E_\varepsilon}{r_{s0}} + \left(\frac{\rho_s}{(\rho_s - r_s)} + \frac{E_T\left(\rho_s(1-T^*) + T^* r_s\right)}{r_s^2} \right) \frac{\phi P}{(\rho_s - r_s)} - \frac{E_T E_\varepsilon}{r_s^2}\left(\frac{r_{s0} - r_s}{r_{s0}} \right) + \frac{E_T^2}{r_s^2}\left(\frac{E_s}{r_s} - \frac{E_{s0}}{r_{s0}} - \frac{m_s^2}{2r_s^2} + \frac{m_{s0}^2}{2r_{s0}^2} \right) \tag{22}$$

The corresponding right eigenvectors, $\mathbf{R}^k$, were found to be

$$R^1 = \begin{bmatrix} 0 \\ 1 \\ 0 \\ V_s - a_s \\ 0 \\ H_s - V_s a_s \end{bmatrix}, \quad R^2 = \begin{bmatrix} 1 \\ -\dfrac{a_f^2(\rho_s - (\rho_s - r_s)T^*)}{(a_s^2 - \vartheta_1^2)(\rho_s - r_s)T^*} \\ V_f - a_f \\ \dfrac{a_f^2(\rho_s - (\rho_s - r_s)T^*)(\vartheta_1 - V_s)}{(a_s^2 - \vartheta_1^2)(\rho_s - r_s)T^*} \\ H_f - V_f a_f \\ \dfrac{a_f^2(\rho_s - (\rho_s - r_s)T^*)(\vartheta_1 V_s - H_s)}{(a_s^2 - \vartheta_1^2)(\rho_s - r_s)T^*} \end{bmatrix}, \quad R^3 = \begin{bmatrix} 0 \\ 1 \\ 0 \\ V_s \\ 0 \\ H_s - \dfrac{r_s a_s^2}{E_T} \end{bmatrix}$$

$$R^4 = \begin{bmatrix} 1 \\ 0 \\ V_f \\ 0 \\ V_f^2 \\ 0 \end{bmatrix}, \quad R^5 = \begin{bmatrix} 1 \\ -\dfrac{a_f^2(\rho_s - (\rho_s - r_s)T^*)}{(a_s^2 - \vartheta_2^2)(\rho_s - r_s)T^*} \\ V_f + a_f \\ -\dfrac{a_f^2(\rho_s - (\rho_s - r_s)T^*)(\vartheta_2 + V_s)}{(a_s^2 - \vartheta_2^2)(\rho_s - r_s)T^*} \\ H_f + V_f a_f \\ -\dfrac{a_f^2(\rho_s - (\rho_s - r_s)T^*)(\vartheta_2 V_s + H_s)}{(a_s^2 - \vartheta_2^2)(\rho_s - r_s)T^*} \end{bmatrix}, \quad R^6 = \begin{bmatrix} 0 \\ 1 \\ 0 \\ V_s + a_s \\ 0 \\ H_s + V_s a_s \end{bmatrix} \tag{23}$$

where

$$H_f = \frac{E_f + T_f^* \phi P}{r_f} \tag{24}$$

and

$$H_s = \frac{E_s}{r_s} - E_\varepsilon\left(\frac{r_{s0} - r_s}{r_s r_{s0}} \right) + \frac{E_T}{r_s}\left(\frac{E_s}{r_s} - \frac{E_{s0}}{r_{s0}} - \frac{m_s^2}{2r_s^2} + \frac{m_{s0}^2}{2r_{s0}^2} \right) + \frac{(1 - \phi T^*)P}{r_s} \tag{25}$$

are the enthalpies of the fluid and the solid phases respectively. ϑ_1 and ϑ_2 are defined by

$$\vartheta_1 = a_f - V_f + V_s$$

and

$$\vartheta_2 = a_f + V_f - V_s \tag{26}$$

The parameters $a^k_{j+1/2}$ were obtained by solving the following linear equations

$$U_{j+1} - U_j = \sum_{k=1}^{6} \alpha^k_{j+1/2} R^k_{j+1/2} \tag{27}$$

to be

$$\begin{aligned}
&\alpha^1_{j+1/2} = (C_3 - C_4)/2 \\
&+ \frac{(\rho_s - (\rho_s - \hat{r}_s)T^*)\hat{a}_f^2\left(\left(\hat{a}_s + \hat{V}_f - \hat{V}_s\right)C_1 - \hat{a}_f C_2\right)}{2(\rho_s - \hat{r}_s)T^*\hat{a}_s\left(\hat{a}_s - \hat{\vartheta}_1\right)\left(\hat{a}_s + \hat{\vartheta}_2\right)}, \\
&\alpha^2_{j+1/2} = (C_1 - C_2)/2, \qquad \alpha^3_{j+1/2} = [r_s] - C_3, \\
&\alpha^4_{j+1/2} = [r_f] - C_1, \qquad \alpha^5_{j+1/2} = (C_1 + C_2)/2, \\
&\alpha^6_{j+1/2} = (C_3 + C_4)/2 \\
&+ \frac{(\rho_s - (\rho_s - \hat{r}_s)T^*)\hat{a}_f^2\left(\left(\hat{a}_s - \hat{V}_f + \hat{V}_s\right)C_1 + \hat{a}_f C_2\right)}{2(\rho_s - \hat{r}_s)T^*\hat{a}_s\left(\hat{a}_s + \hat{\vartheta}_1\right)\left(\hat{a}_s - \hat{\vartheta}_2\right)}.
\end{aligned} \tag{28}$$

where $[b] \equiv b_{j+1} - b_j$, $\hat{b}$ is an average property in the interval $[x_{j+1} - x_j]$ and the parameters C_k (for $k = 1, 2, 3, 4$) are as follows:

$$\begin{aligned}
C_1 &= \frac{(\gamma - 1)T^*\left([E_f] + \frac{1}{2}\hat{V}_f^2[r_f] - \hat{V}_f[m_f]\right)}{\hat{a}_f^2}, \qquad C_2 = \frac{[m_f] - \hat{V}_f[r_f]}{\hat{a}_f} \\
C_3 &= \frac{E_T\left([E_s] + \left(\hat{V}_s^2 - \hat{H}_s + \frac{\hat{r}_s\hat{a}_s^2}{E_T}\right)[r_s] - \hat{V}_s[m_s]\right)}{\hat{r}_s\hat{a}_s^2}, \quad C_4 = \frac{[m_s] - \hat{V}_s[r_s]}{\hat{a}_s}
\end{aligned} \tag{29}$$

The boundary condition on the shock-tube end-wall was simulated by using the image point method. The computational grid system was composed of 500 nodes. The computations were performed with DecStation 5000/260 and Indy R4400/150.

Numerical results

The shock tube problem in pure gases – code validation

The performance of the presently developed TVD scheme was checked by simulating the well known 1-D shock tube problem which is schematically

shown in Figure 1(a). Figure 2 illustrates the analytical solution (solid lines) and the numerical predictions (open circles) for the fluid's density, velocity and pressure distributions. The initial conditions for this simulation were:

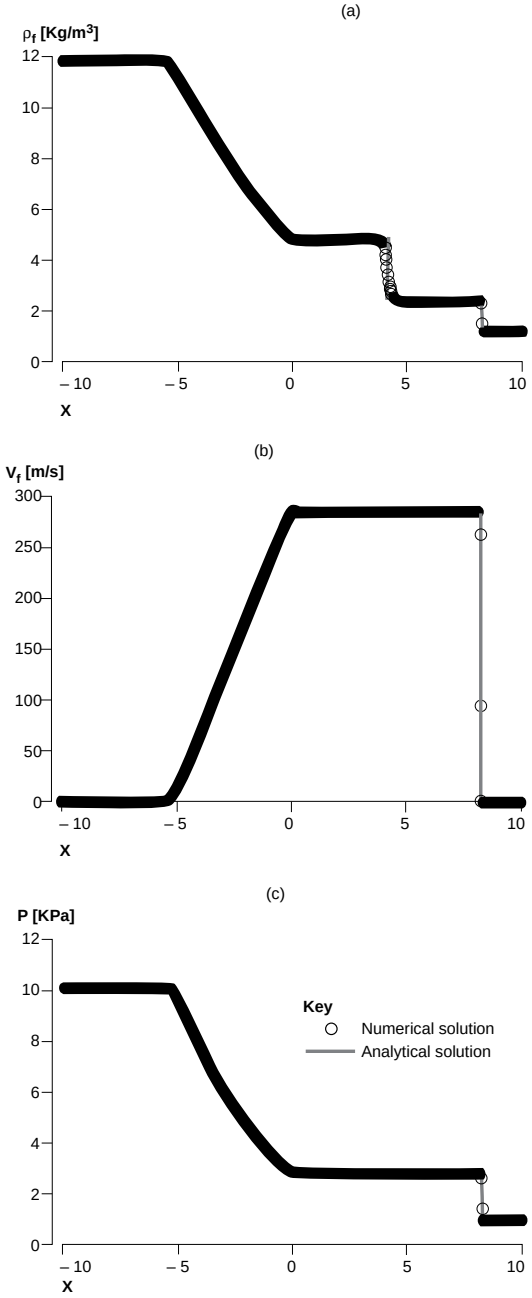

Figure 2. Comparison between the analytical and the numerical solutions of the problem show in Figure 1(a): (a) the density field (b) the velocity field (c) the pressure field

$$U(x) = \begin{cases} U_L, & x \le 0 \\ U_R, & x > 0 \end{cases}$$

where

$$U_L = \begin{bmatrix} r_f \\ r_s \\ m_f \\ m_s \\ E_f \\ E_s \end{bmatrix}_L = \begin{bmatrix} 11.7683 \\ 0 \\ 0 \\ 0 \\ 2533125 \\ 0 \end{bmatrix}, \qquad U_R = \begin{bmatrix} r_f \\ r_s \\ m_f \\ m_s \\ E_f \\ E_s \end{bmatrix}_R = \begin{bmatrix} 1.17683 \\ 0 \\ 0 \\ 0 \\ 253312.5 \\ 0 \end{bmatrix}$$

The comparison between the analytical solutions and the numerical predictions of the present simulation clearly indicates that the presently developed TVD-based numerical code reproduces the 1-D shock tube problem excellently.

The shock tube problem in porous media

Once the code was validated it was used to solve the problem shown in Figure 1(b), in which the media in both sides of the diaphragm were porous. The results of this simulation for a variety of properties are shown in Figures 3(a)-3(f). Two different cases are shown in each of these figures. The solid lines correspond to the distribution of the property 130μs after the diaphragm rupture for a porous material sample having a length of 40cm, and the dashed lines correspond to the distribution of the property 260μs after the diaphragm rupture for a porous material sample having a length of 80cm. Had the problem been self-similar, the solid and the dashed lines should have been perfectly overlapping each other. Consequently, the fact that they do not overlap each other indicates that the problem is not self-similar. However, an inspection of Figures 3(a)-3(c) indicates that the fluid pressure, P, the fluid density, ρ_f, and the porosity, ϕ, can be considered as self-similar from an engineering point of view. The solid stress, σ_s, the solid velocity, V_s, and the fluid velocity, V_f, whose distributions are shown in Figures 3(d)-3(f), clearly reveal that they could not be assumed to be self-similar even from an engineering point of view. While the differences in P, ρ_f and ϕ between the two cases are negligibly small, the differences in σ_s, V_s and V_f are 20 per cent to 30 per cent.

It is important to note here that the flow field is not self-similar, in spite of the fact that the compaction waves were found to propagate at constant velocities. This numerical finding was supported experimentally by Sandursky and Liddiard (1985) and Levy *et al.* (1993b).

Conclusions

The Riemann problem inside a porous medium has been solved numerically using a TVD-based code which was especially developed by us for this

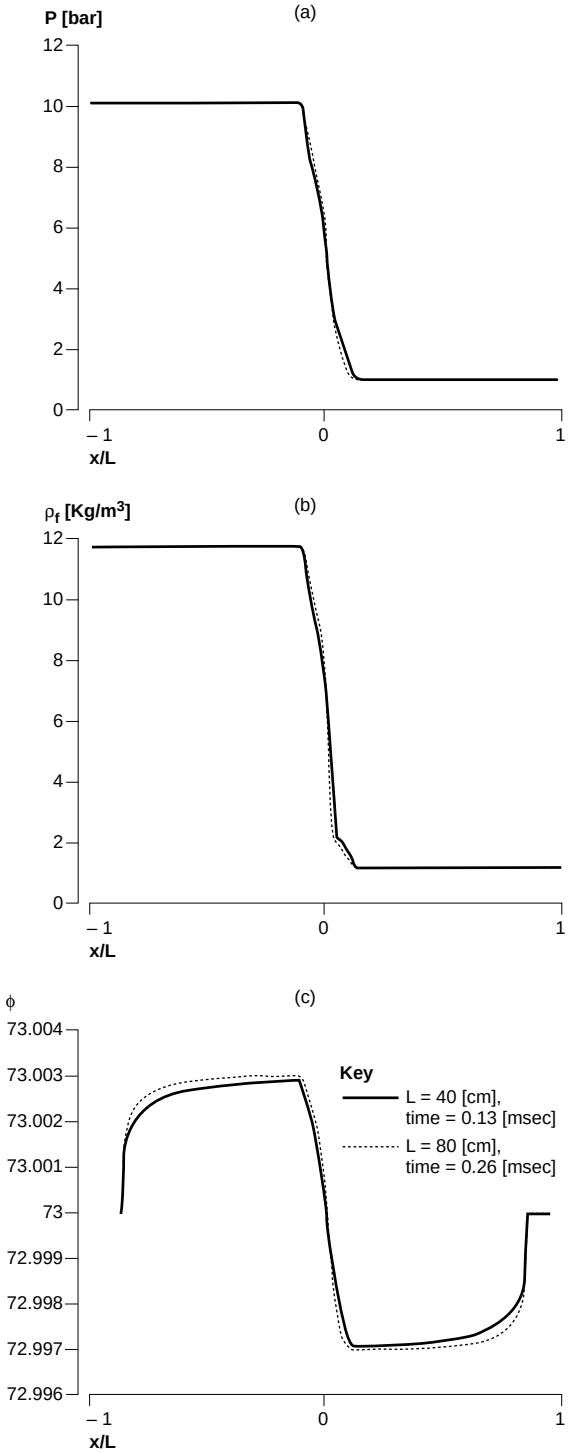

Figure 3.
Numerical solution of the problem show in Figure 1(b): (a) the pressure field (b) the fluid density field (c) the porosity field (d) the solid normal stress field (e) the solid velocity field (f) the fluid velocity field

(*Continued*)

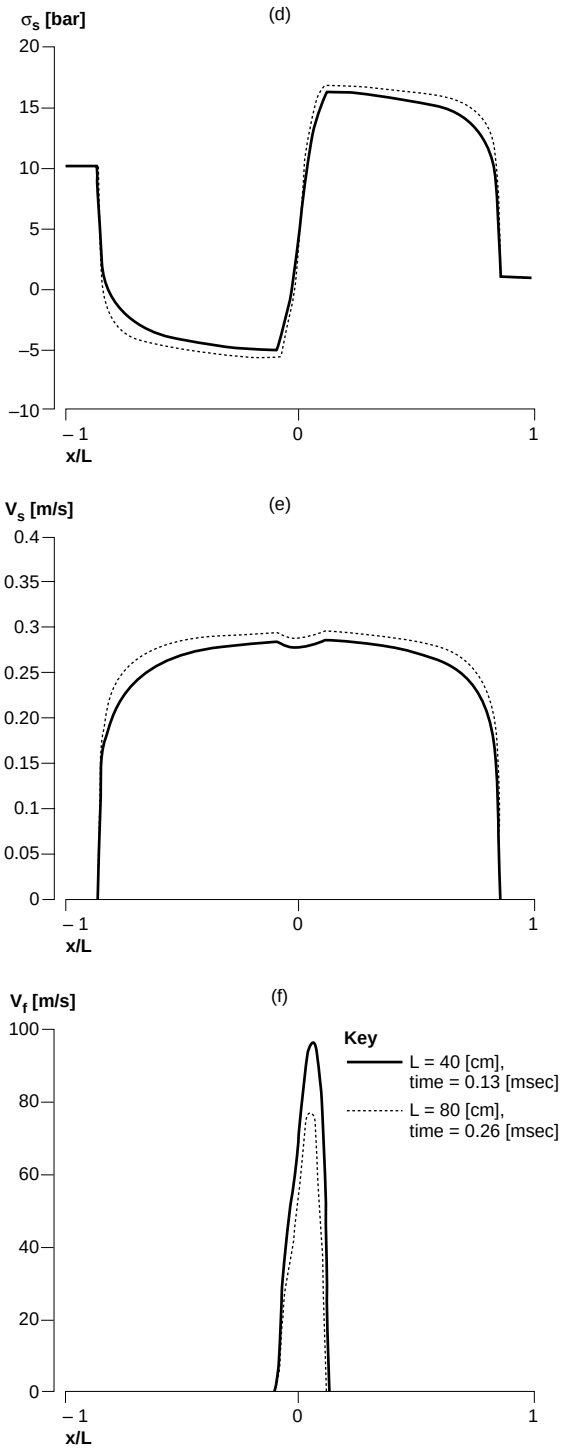
(d)
σs [bar]
20
15
10
5
0
–5
–10
– 1
0
1
x/L
(e)
Vs [m/s]
0.4
0.35
0.3
0.25
0.20
0.15
0.1
0.05
0
– 1
0
1
x/L
(f)
Vf [m/s]
100
80
60
40
20
0
– 1
0
1
x/L
Key
L = 40 [cm],
time = 0.13 [msec]
L = 80 [cm],
time = 0.26 [msec]

Figure 3.

purpose. It has been shown that the resulting flow field is, in general, not self-similar. However, the pressure, the fluid density and the porosity distributions were found to be practically close to being self-similar. Owing to the technical difficulty of rupturing the diaphragm which separates the high and the low pressure chambers, such a problem cannot be set up in a conventional shock tube. Consequently, the present study should be considered as a theoretical one.

However, to the best of the authors' knowledge, this is the first time that the Riemann problem has been solved inside a porous medium.

Note

1. We use the term "rigid" in the loose relative sense which is common when applied to porous materials, in general, and foams, in particular, i.e. that deformations do not exceed a few percent.

References

Bear, J. and Bachmat, Y. (1990), *Introduction to Modelling of Transport Phenomena in Porous Media,* Kluwer Academic Publishers, Dordrecht, Germany.

Bear, J., Sorek, S., Ben-Dor, G. and Mazor, G. (1992), "Displacement waves in saturated thermo-elastic porous media. I. Basic equations", *Fluid Dynamic Research,* Vol. 9, pp. 155-64.

Harten, A. (1983), "High resolution schemes for hyperbolic conservation laws", *Journal of Computational Physics*, Vol. 49, pp. 357-93.

Krylov, A., Sorek, S., Levy, A. and Ben-Dor, G. (1996), "Simple waves in saturated porous media. I. the isothermal case", *Japan Society of Mechanical Engineers International Journal*, Ser. B, Vol. 39 No. 2, pp. 294-8.

Levy, A. (1995), "Wave propagation in a saturated porous media", PhD thesis, Department of Mechanical Engineering, Ben-Gurion University of the Negev, Beer Sheva, Israel (in Hebrew).

Levy, A., Ben-Dor, G., Sorek, S. and Bear, J. (1993a), "Jump conditions across strong compaction waves in gas saturated rigid porous media", *Shock Waves*, Vol. 3 No. 2, pp. 105-11.

Levy, A., Ben-Dor, G., Skews, B. and Sorek, S. (1993b), "Head-on collision of normal shock waves with rigid porous materials", *Experiments in Fluids*, Vol. 15, pp. 183-90.

Levy, A., Sorek, S., Ben-Dor, G. and Bear, J. (1995a), "Evolution of the balance equations in saturated thermoelastic porous media following abrupt simultaneous changes in pressure and temperature", *Transport in Porous Media*, Vol. 21, pp. 241-68.

Levy, A., Sorek, S., Ben-Dor, G. and Skews, B. (1995b), "Waves propagation in saturated rigid porous media: analytical model and comparison with experimental results", *Fluid Dynamic Research*, Vol. 17, pp. 49-65.

Levy, A., Sorek, S. and Ben-Dor, G. (1996), "Numerical investigation of the propagation of shock waves in rigid porous materials: Part I – development of the computer code and comparison with experimental results" (submitted for publication)

Sandusky, H.W., and Liddiard,T.P. (1985), "Dynamic compaction of porous beds", NSWC TR 83-256, NAVAL Surface Weapons Center, White Oak, MD.

Sorek, S., Bear, J., Ben-Dor, G. and Mazor, G. (1992), "Shock waves in saturated thermoelastic porous media", *Transport in Porous Media,* Vol. 9, pp. 3-13.

Sorek, S., Krylov, A., Levy, A. and Ben-Dor, G. (1995), "Simple waves in saturated porous media. II. the nonisothermal case", *Japan Society of Mechanical Engineers International Journal*, Ser. B, Vol. 39, pp. 299-304.